

---

---

MICROCRYSTALLINE, NANOCRYSTALLINE, POROUS,  
AND COMPOSITE SEMICONDUCTORS

---

---

## Structural Studies of ZnS:Cu (5 at %) Nanocomposites in Porous Al<sub>2</sub>O<sub>3</sub> of Different Thicknesses

R. G. Valeev<sup>a\*</sup>, A. L. Trigub<sup>a, b</sup>, A. I. Chukavin<sup>a</sup>, and A. N. Beltiukov<sup>a</sup>

<sup>a</sup> *Physical-Technical Institute, Russian Academy of Sciences (Ural Branch), Izhevsk, 426000 Russia*

<sup>b</sup> *National Research Center “Kurchatov Institute”, Moscow, 123182 Russia*

\**e-mail: rishatvaleev@mail.ru*

Submitted June 6, 2016; accepted for publication June 16, 2016

**Abstract**—We present EXAFS, XANES, and X-ray diffraction data on nanoscale ZnS:Cu (5 at %) structures fabricated by the thermal deposition of a ZnS and Cu powder mixture in porous anodic alumina matrices with a pore diameter of 80 nm and thicknesses of 1, 3, and 5 μm. The results obtained are compared with data on ZnS:Cu films deposited onto a polycor surface. According to X-ray diffraction data, the samples contain copper and zinc compounds with sulfur (Cu<sub>2</sub>S and ZnS, respectively); the ZnS compound is in the cubic (sphalerite) and hexagonal (wurtzite) modifications. EXAFS and XANES studies at the *K* absorption edges of zinc and copper showed that, in samples deposited onto polycor and alumina with thicknesses of 3 and 5 μm, most copper atoms form the Cu<sub>2</sub>S compound, while, in the sample deposited onto a 1-μm-thick alumina layer, copper atoms form metallic particles on the sample surface. Copper crystals affect the Zn–S interatomic distance in the sample with a 1-μm-thick porous Al<sub>2</sub>O<sub>3</sub> layer; this distance is smaller than in the other samples.

DOI: 10.1134/S1063782617020221

### 1. INTRODUCTION

As is well-known, the light-technical characteristics of electroluminescent light sources based on zinc sulfide doped with different elements heavily depend on the thickness and structure of the luminophor layer and uniformity of the dopant distribution [1]. In thin-film electroluminescent light sources (ELs), doping can be performed either during growth of the luminophor layer, e.g., by thermal annealing in vacuum in the presence of dopant atoms [2] or by the deposition of doped zinc sulphide [3]. Copper with its ability to segregate to the surface has the highest concentration in a (2–3)-nm-thick layer, but deeper in the sample, the Cu concentration equalizes [4].

Porous anodic alumina (AA) with the hexagonal ordering of pores oriented vertically with respect to the film surface has been widely used as a matrix in the synthesis of various nanostructures, including nanowires, nanodots, nanorings, nanotubes, and so on [5, 6]. Anodic alumina can be successfully used as a carrier of catalytically active nanoparticles [7] and semiconductor nanostructures [5, 8]. It allows the formation of ordered arrays of semiconductor luminophor nanostructures with the same sizes and shapes, so each nanostructure can be presented as a separate light emitter. Coherent summation of the radiation from each source will significantly enhance the light intensity [9].

As was mentioned above, the light-related characteristics of ELs depend on the thickness and structure of the luminophor layer. In the ELs formed from semiconductor–insulator matrix nanocomposites, the matrix-layer thickness also plays an important role. The depth of continuous pore sputtering is approximately equal to the pore diameter, but the deposited material penetrates into the matrix pores to a depth of up to 10 μm and forms nanoparticles on the pore walls [10, 11]. As a result, the mechanisms of nanostructure growth in matrices of different thicknesses can be different and the structures of the luminophor formed by thermal deposition of the powder mixture can be different as well. This requires investigations using different structure-sensitive techniques, such as X-ray diffraction (XRD), extended X-ray absorption fine structure (EXAFS) and X-ray absorption near edge structure (XANES) spectroscopies.

Therefore, this study is aimed at carrying out XRD, EXAFS, and XANES investigations of ZnS:Cu + Al<sub>2</sub>O<sub>3</sub> nanocomposite systems with AA porous matrix thicknesses of 1, 3, and 5 μm to select the optimal thickness of the emitting layer for the fabrication of ELs with the highest emission performances.

### 2. EXPERIMENTAL

Porous AA matrices were synthesized by the two-stage anodic oxidation of aluminum wafers (99.99%)

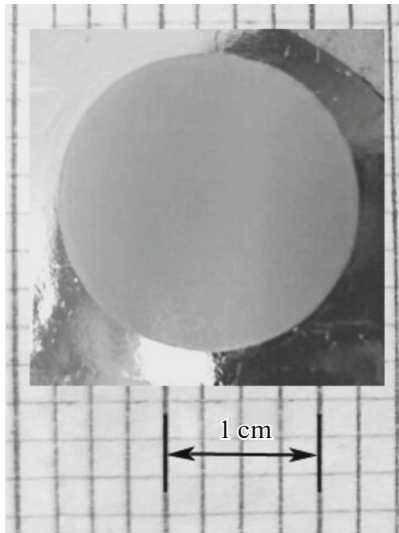


**Fig. 1.** Photograph of a typical AA matrix formed by two-stage anodic oxidation of an aluminum wafer.

at a fixed voltage of 80 V [12]. Lin et al. [13] observed that, regardless of the electrolyte concentration and anodizing voltage, the flowing of electric charge of 2 C through a surface with an area of 1 cm<sup>2</sup> results in the growth of an alumina film with a thickness of 1 μm. In the case under consideration, the surface area was 3.14 cm<sup>2</sup>, which corresponds to a diameter of 20 mm (Fig. 1). The quantity of electric charge flowing through the sample was programmably controlled with an AKIP-1134-300-5 power source used for synthesis. Matrices with thicknesses of 1, 3, and 5 μm were formed using electric charges of 6.3, 18.9, and 31.4 C, respectively.

Samples of copper-doped (5 at %) zinc sulphide deposited onto a porous AA surface were fabricated by the thermal evaporation of ZnS and CuS powder mixture in high vacuum (no lower than 10<sup>-5</sup> Pa) [4].

XRD investigations of the structure and phase state of the samples were carried out at the station “Structural Materials Science”, Kurchatov Synchrotron Radiation Center (KSRC), National Research Center “Kurchatov Institute”. X-ray radiation with a wavelength of 0.68886 Å was used for excitation. The diffraction patterns were identified using the JSPDS database.

The EXAFS investigations were also carried out at the station “Structural Materials Science”, KSRC in the fluorescence yield mode. A Si (111) crystal was used to provide monochromatization of the incident radiation. The EXAFS spectra were obtained at the *K* absorption edges of zinc (the energy  $E_K = 9659$  eV) and copper (the energy  $E_K = 8979$  eV). Experimental data were analyzed using the Iffefit program package [14]. Information on the structure was obtained from X-ray spectra using the standard procedure, which included

subtraction of the pre- and post-edge background and normalization of the spectrum to the absorption jump. The pseudo-radial function of the distribution of atoms near the absorbing one was obtained by the Fourier transform. The interatomic distances  $R_i$ , coordination numbers  $N_i$ , and Debye–Waller parameters  $\sigma_i^2$  for each  $i_{th}$  coordination sphere were determined by nonlinear fitting of the theoretical spectrum to the experimental one using the formula for the EXAFS function

$$\chi(k) = S_0^2 \times \sum_{i=1}^n \frac{N_i F_i(k)}{R_i^2 k} e^{-2R_i/\lambda(k)} e^{-2\sigma_i^2 k^2} \sin[2kR_i + \varphi_i(k)].$$

The theoretical data were calculated using the free path length  $\lambda(k)$  of a photoelectron with the wave vector  $k$ , amplitude  $F_i(k)$ , and phase shifts  $\varphi_i(k)$  ab initio calculated using the FEFF6 program package [15].

### 3. RESULTS AND DISCUSSION

Figure 2 shows X-ray diffraction patterns of the samples with different AA matrix thicknesses in the angle range of  $2\theta = 17\text{--}24^\circ$  in comparison with the diffraction pattern of the polycor substrate surface. The diffraction pattern contains peaks of cubic (sphalerite) and hexagonal (wurtzite) ZnS phases (ZnS-*s* and ZnS-*w*, respectively) and of the Cu<sub>2</sub>S compound with the digenite crystal structure. The diffraction pattern of the sample with a 1-μm-thick matrix includes also Al and Cu peaks. The occurrence of the Al peak is related to the features of sample preparation for the analysis, during which the anodic layer was scraped off from the aluminum substrate surface to form a powder (powder diffractometry at the station “Structural Materials Science”, KSRC). Scraping off the material from the samples with a thicker matrix for analysis does not lead to the occurrence of aluminum reflections in the diffraction patterns.

The occurrence of the Cu diffraction line is related to the mechanisms of penetration of a material into pores in the matrix. The material is deposited to a depth of up to 10 μm, but, in this case, due to the small matrix thickness, ZnS:Cu forms at small depths and copper segregates to the surface without bonding with sulphur and forms copper particles. In addition, we note that this result is indicative of the decomposition of CuS during evaporation.

Figure 3 presents normalized oscillating portions of the X-ray absorption spectra and their Fourier transforms (FTs) for the *K* absorption edge of zinc. The vertical line shows the position of the maximum corresponding to the Zn–S chemical bond of undoped zinc

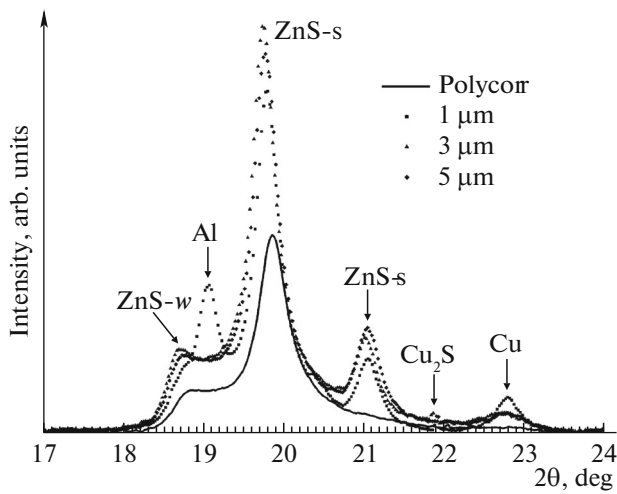


**Fig. 2.** X-ray diffraction patterns of the ZnS:Cu (5 at %) + Al<sub>2</sub>O<sub>3</sub> samples formed by deposition onto matrices with a pore diameter of 80 nm and a thickness of 1, 3, and 5 μm in comparison with the patterns of the film on polycorr.

sulphide (2.338 Å). Numerical values of the parameters of the local atomic environment of zinc atoms obtained by Fourier fitting are listed in Table 1. It can be seen that, with increasing thickness of the porous Al<sub>2</sub>O<sub>3</sub> matrix, the Zn–S, *R* chemical-bond length

increases; in this case, the number *N* of sulphur atoms around zinc atoms is invariable within fitting error.

The normalized oscillating portions of the X-ray absorption spectra and their FTs for the *K* absorption edge Cu are presented in Fig. 4. Vertical lines show the positions of maxima corresponding to the Cu–S chemical bonds in the Cu<sub>2</sub>S compound and to the Cu–Cu bond in pure copper. The numerical values of the parameters of the local atomic environment of copper atoms obtained by Fourier fitting are given in Table 2. In the sample with a matrix thickness of 1 μm, the FT peak corresponds to the position of the Cu–Cu chemical bond, which indicates that the copper phase segregates on the sample surface, while for the rest of the samples, including the film on the polycorr surface, the position of the maximum corresponds to the Cu–S bond.

Figure 5 shows the curves of X-ray absorption near-edge fine structure (XANES). Vertical lines show spectral features whose positions can be affected by the chemical states of atoms in the local environment of the absorbing atom. The spectra at the *K* edge of zinc show that the maximum near 9701 eV in curve 3 corresponding to the ZnS:Cu sample deposited onto a 1-μm-thick matrix shifts to the right in comparison with the data for other samples. This allows us to conclude that the Zn–S distance in the sample with a

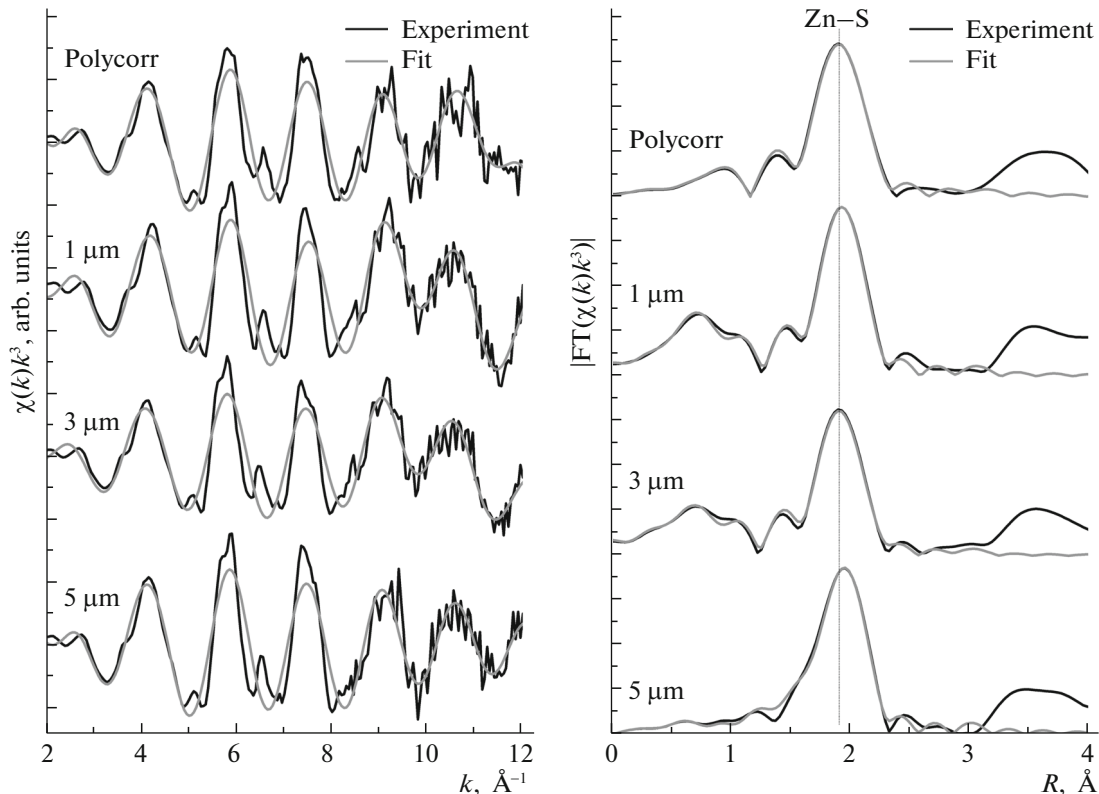


**Fig. 3.** Normalized oscillating portions of EXAFS spectra and their Fourier transforms at the *K* absorption edge of zinc.

**Table 1.** Parameters of the local atomic environment of zinc atoms

Sample	Zn-S		
	$R, \text{\AA}$	$N$	$\sigma^2, \text{\AA}^2$
Polycorr	$2.350 \pm 0.005$	$3.5 \pm 0.5$	$0.005 \pm 0.001$
AA, 1 $\mu\text{m}$	$2.347 \pm 0.005$	$3.8 \pm 0.5$	$0.005 \pm 0.001$
AA, 3 $\mu\text{m}$	$2.350 \pm 0.005$	$3.9 \pm 0.5$	$0.005 \pm 0.001$
AA, 5 $\mu\text{m}$	$2.354 \pm 0.005$	$4.1 \pm 0.5$	$0.005 \pm 0.001$

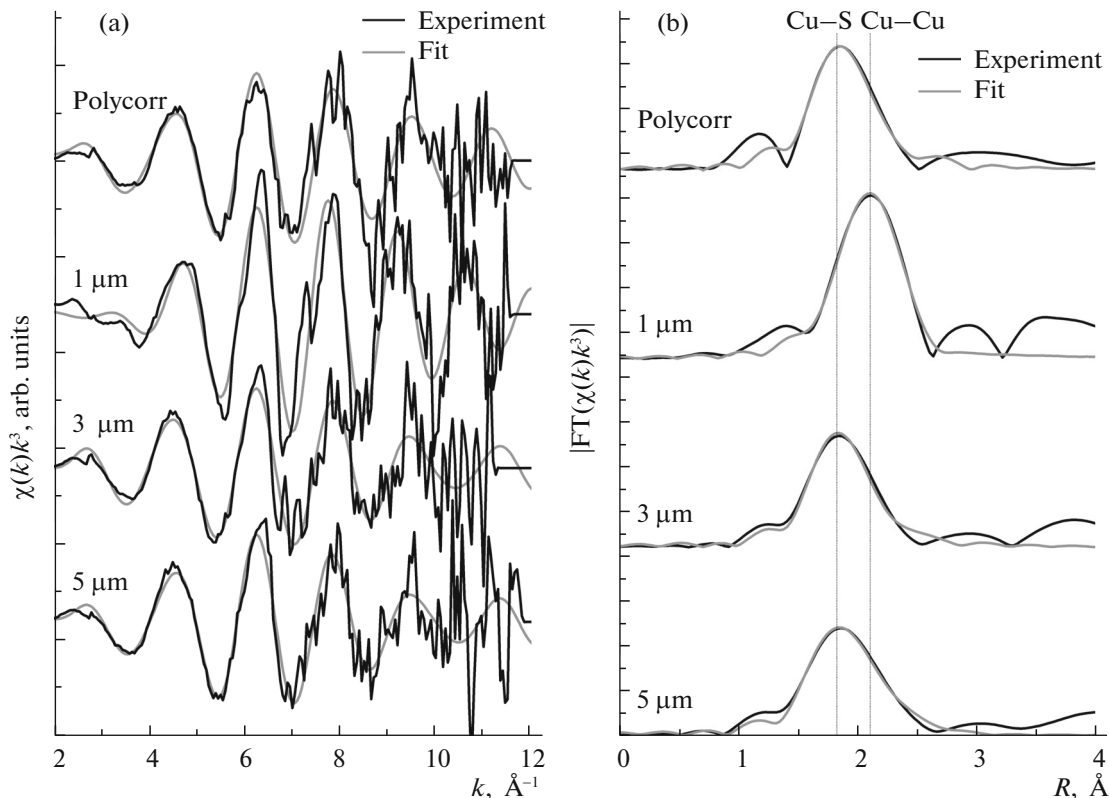
**Table 2.** Parameters of the local atomic environment of copper atoms

Sample	Cu-S			Cu-Cu		
	$R, \text{\AA}$	$N$	$\sigma^2, \text{\AA}^2$	$R, \text{\AA}$	$N$	$\sigma^2, \text{\AA}^2$
Polycorr	$2.24 \pm 0.01$	$2.5 \pm 0.5$	$0.004 \pm 0.001$	$2.53 \pm 0.01$	$2.5 \pm 0.5$	$0.021 \pm 0.001$
AA, 1 $\mu\text{m}$	$2.20 \pm 0.01$	$0.8 \pm 0.5$	$0.004 \pm 0.001$	$2.49 \pm 0.01$	$7.0 \pm 0.5$	$0.009 \pm 0.001$
AA, 3 $\mu\text{m}$	$2.23 \pm 0.01$	$2.4 \pm 0.5$	$0.003 \pm 0.001$	$2.54 \pm 0.01$	$1.3 \pm 0.5$	$0.007 \pm 0.001$
AA, 5 $\mu\text{m}$	$2.23 \pm 0.01$	$2.3 \pm 0.5$	$0.004 \pm 0.001$	$2.55 \pm 0.01$	$2.1 \pm 0.5$	$0.010 \pm 0.001$

1- $\mu\text{m}$ -thick matrix decreases relative to the other samples, which agrees well with the EXAFS data.

The XANES spectrum obtained at the  $K$  absorption edge of copper for the sample with a 1- $\mu\text{m}$ -thick matrix differs from the spectra for the samples on

polycorr and matrices with a thickness of 3 and 5  $\mu\text{m}$ . The positions of the spectral peaks for this sample coincide with the positions of the peaks in the copper-foil spectrum. Along with the EXAFS and X-ray data, this confirms the conclusion about the presence of

**Fig. 4.** (a) Normalized oscillating portions of EXAFS spectra and (b) their Fourier transforms at the  $K$  absorption edge of copper.

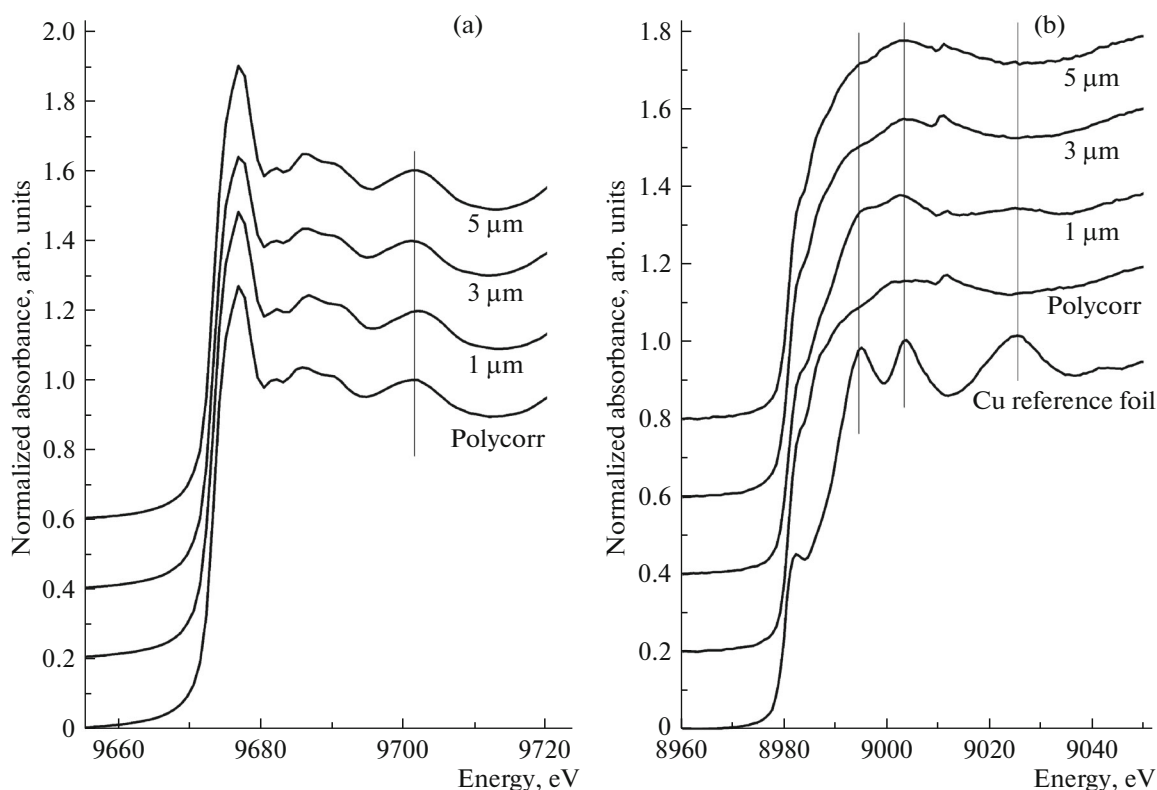


Fig. 5. XANES spectra obtained at the absorption edges of (a) Zn and (b) Cu.

copper in the form of metallic nanoparticles on the surface of this sample. The spectra of the samples on polycorr and alumina with thicknesses of 3 and 5  $\mu\text{m}$  are identical; consequently, the copper state in these samples is the same.

#### 4. CONCLUSIONS

Thus, in this publication, we presented the EXAFS, XANES, and X-ray data on nanoscale ZnS:Cu (5 at %) structures formed by the thermal deposition of a ZnS and Cu powder mixture in porous anodic alumina matrices with a pore diameter of 80 nm and thicknesses of 1, 3, and 5  $\mu\text{m}$ . The results obtained were compared with data on ZnS:Cu films deposited onto a polycorr surface. X-ray analysis of the samples showed the presence of copper and zinc compounds with sulphur ( $\text{Cu}_2\text{S}$  and ZnS, respectively); the ZnS compound is in the cubic (sphalerite) and hexagonal (wurtzite) modifications. The EXAFS and XANES investigations at the  $K$  absorption edges of zinc and copper showed that, in the samples deposited onto polycorr and alumina with thicknesses of 3 and 5  $\mu\text{m}$ , most copper atoms are in the  $\text{Cu}_2\text{S}$  compound, while, in the sample deposited onto the 1- $\mu\text{m}$ -thick alumina layer, copper atoms form metallic particles on the sample surface. This is related to the mechanism of penetration of the material into the matrix pores: the

material is deposited to a depth of up to 10  $\mu\text{m}$ , but in this case, due to the small thickness of the matrix, ZnS:Cu forms at small depths and copper segregates to the surface without bonding with sulphur. The presence of copper crystals affects the Zn–S interatomic distance for the sample with a porous  $\text{Al}_2\text{O}_3$  layer thickness of 1  $\mu\text{m}$ : this distance is smaller than that in the other samples.

#### ACKNOWLEDGMENTS

This study was supported by the Russian Science Foundation, project no. 15-19-10002.

#### REFERENCES

1. O. V. Maksimova and M. K. Samokhvalov, *Development of Analysis and Synthesis Methods of Thin Film Electroluminescent Elements in Indicator Devices* (Ul'yan. Gos. Tekh. Univ., Ul'yanovsk, 2010), Chap. 2, p. 26 [in Russian].
2. Yu. Yu. Bacherikov and N. V. Kitsyuk, *Tech. Phys.* **50**, 658 (2005).
3. I. K. Vereshchagin, B. A. Kovalev, L. A. Kosyachenko, and S. M. Kokin, *Electroluminescent Light Sources* (Energoatomizdat, Moscow, 1990), Chap. 3, p. 87 [in Russian].

4. R. G. Valeev, D. I. Petukhov, A. I. Chukavin, and A. N. Beltukov, *Semiconductors* **50**, 266 (2016).
5. X. Fang, T. Zhai, U. K. Gautam, L. Li, L. Wu, Y. Bando, and D. Goldberg, *Prog. Mater. Sci.* **56**, 175 (2011).
6. C. T. Sousa, D. C. Leitao, M. P. Proenca, J. Ventura, A. M. Pereira, and J. P. Araujo, *Appl. Phys. Rev.* **1**, 031102 (2014).
7. F. Bentaleb and E. Marceau, *Microporous Mesoporous Mater.* **156**, 40 (2012).
8. R. Valeev, E. Romanov, A. Beltukov, V. Mukhgalin, I. Roslyakov, and A. Eliseev, *Phys. Status Solidi C* **9**, 1462 (2012).
9. D. Botez and D. R. Scifres, *Diode Laser Arrays* (Cambridge Univ. Press, Cambridge, 2005), p. 411.
10. R. G. Valeev, D. V. Surnin, A. N. Bel'tyukov, V. M. Vetoshkin, V. V. Kriventsov, Ya. V. Zubavichus, A. A. Eliseev, and N. A. Mezentsev, *J. Struct. Chem.* **51**, S132 (2010).
11. A. Beltukov, R. Valeev, E. Romanov, and V. Mukhgalin, *Phys. Status Solidi C* **11**, 1452 (2014).
12. D. I. Petukhov, K. S. Napol'skii, M. V. Berekchiyan, A. G. Lebedev, and A. A. Eliseev, *ACS Appl. Mater. Interfaces* **5**, 7819 (2013).
13. Y. Lin, Q. Lin, X. Liu, Y. Gao, J. He, W. Wang, and Z. Fan, *Nanoscale Res. Lett.* **10**, 495 (2015).
14. M. Newville, *J. Synchrotr. Rad.* **8**, 322 (2001).
15. S. I. Zabinsky, J. J. Rehr, A. Ankudinov, R. C. Albers, and M. J. Eller, *Phys. Rev. B* **52**, 2995 (1995).

*Translated by E. Bondareva*